Universiteit Antwerpen

This item is the archived peer-reviewed author-version of:

Effect of substitutional impurities on the electronic transport properties of graphene

Reference:
Berdiyorov G. R., Bahlouli H., Peeters François.- Effect of substitutional impurities on the electronic transport properties of graphene
Physica. E: Low-dimensional systems and nanostructures - ISSN 1386-9477 - 84(2016), p. 22-26
Full text (Publisher's DOI): https://doi.org/10.1016/J.PHYSE.2016.05.024
To cite this reference: http://hdl.handle.net/10067/1356990151162165141

uantwerpen.be
Institutional repository IRUA

Author's Accepted Manuscript

Effect of substitutional impurities on the electronic transport properties of graphene

G.R. Berdiyorov, H. Bahlouli, F.M. Peeters

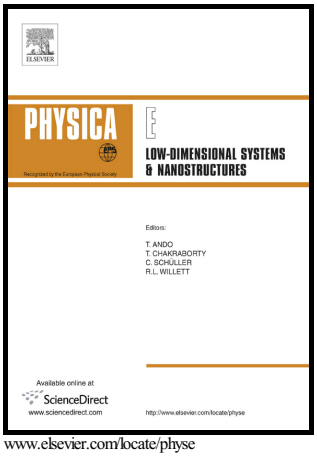

www.elsevier.com/locate/physe

PII: S1386-9477(16)30449-0
DOI: http://dx.doi.org/10.1016/j.physe.2016.05.024
Reference: PHYSE12454

To appear in: *Physica E: Low-dimensional Systems and Nanostructures*

Received date: 1 February 2016
Revised date: 18 May 2016
Accepted date: 19 May 2016

Cite this article as: G.R. Berdiyorov, H. Bahlouli and F.M. Peeters, Effect o substitutional impurities on the electronic transport properties of graphene *Physica E: Low-dimensional Systems and Nanostructures* http://dx.doi.org/10.1016/j.physe.2016.05.024

This is a PDF file of an unedited manuscript that has been accepted fo publication. As a service to our customers we are providing this early version o the manuscript. The manuscript will undergo copyediting, typesetting, an review of the resulting galley proof before it is published in its final citable form Please note that during the production process errors may be discovered whic could affect the content, and all legal disclaimers that apply to the journal pertain

Effect of substitutional impurities on the electronic transport properties of graphene

ACCEPTED MANUSCRIPT

G. R. Berdiyorov,[1,*] H. Bahlouli,[2,3] and F. M. Peeters[4]

[1] *Qatar Environment and Energy Research Institute, Hamad bin Khalifa University, Qatar Foundation, Doha, Qatar*
[2] *Department of Physics, King Fahd University of Petroleum and Minerals, 31261 Dhahran, Saudi Arabia*
[3] *Saudi Center for Theoretical Physics, 31261 Dhahran, Saudi Arabia*
[4] *Departement Fysica, Universiteit Antwerpen, Groenenborgerlaan 171, B-2020 Antwerpen, Belgium*

(Dated: May 24, 2016)

Density-functional theory in combination with the nonequilibrium Green's function formalism is used to study the effect of substitutional doping on the electronic transport properties of hydrogen passivated zig-zag graphene nanoribbon devices. B, N and Si atoms are used to substitute carbon atoms located at the center or at the edge of the sample. We found that Si-doping results in better electronic transport as compared to the other substitutions. The transmission spectrum also depends on the location of the substitutional dopants: for single atom doping the largest transmission is obtained for edge substitutions, whereas substitutions in the middle of the sample give larger transmission for double carbon substitutions. The obtained results are explained in terms of electron localization in the system due to the presence of impurities.

PACS numbers:

I. INTRODUCTION.

Recent advances in experimental fabrication techniques have opened new possibilities to manufacture new low-dimensional materials and to study their fundamental properties. Among those materials, graphene – a monolayer of hexagonally arranged carbon atoms – has attracted a lot of interest in the past few decades due to its unique electronic structure and transport properties [1, 2]. Graphene has the potential to be used for practical applications in the field of electronics and photonics [3, 4]. Graphene is also considered as a promising material for sensor applications (see, Ref. [5] for review) due to its exceptionally high surface-to-volume ratio, high charge carrier conductivity, low contact resistance,[6] and low thermal noise,[7]. In addition, the electronic properties of graphene can further be tuned using external fields, which also increases its potential for practical applications.

Edge and surface modifications with different functional groups are considered as an effective tool in refining structural, thermal, electronic and other measurable properties of pristine graphene [8, 9]. Chemical doping of graphene with foreign atoms is considered as one of the grand challenges for the development of graphene-based devices for multiple applications. In this respect, B and N doping is a common method to tune the properties of graphene [10–12]. Such substitutional doping has a profound effect on the charge carrier transport in graphene. For example, for an ordered location of the dopants, the electronic transport can be significantly enhanced [13, 14]. Charge carrier rectification [17] and negative differential resistive phenomena [14] are also reported for such hybrid systems. The effect of boron and nitrogen substitution on the transport properties of graphene nanoribbons as a function of the defect distance from the edge of the sample was recently analysed for both zig-zag edges [15] and armchair edges [16].

In this work, we use density-functional theory (DFT) in combination with the nonequilibrium Green's function formalism to study the electronic transport properties of zig-zag graphene nanoribbons with substitutional doping with B, N and Si atoms. As an example, we consider single and double substitutions either at the edges of the sample or in the middle of the nanoribbon. We found that Si substitution results in better transmission for both locations of the dopants as compared to the use of other dopants. Depending on the type of dopant, prominent changes are obtained in the transmission spectrum of the system due to the formation of strongly localized electronic states. The response of the system to an applied potential difference is also studied.

II. COMPUTATIONAL DETAILS

As an example, we consider a hydrogen-terminated zig-zag graphene nanoribbon of width 11.37 Å. Single and two carbon atoms are substituted respectively with B, N and Si atoms, where the substitutions are done either at the edge of the sample or in the middle of the sample. All considered samples are first optimized using DFT calculations within the generalized gradient approximation (GGA) of Perdew-Burke-Ernzerhof (PBE) for the exchange-correlation energy [18]. The Brillouin zone sampling was performed using $1\times1\times12$ k-point sampling [19]. The electrostatic potentials were determined on a real-space grid with a mesh cutoff energy of 150 Ry and double-zeta-double-polarized basis sets of local numerical orbitals were employed for all atoms. van der

*Electronic address: gberdiyorov@qf.org.qa

Accepted manuscript

ACCEPTED MANUSCRIPT

Waals interactions were accounted for by using Grimme's DFT-D2 empirical dispersion correction [20] to the PBE. Using the optimized structures, we constructed device geometries (see Fig. 1), which consists of left and right regions and the central (scattering) region (i.e., a two probe configuration). The electrodes are modelled as an electron gas with a fixed chemical potential. The transmission is calculated along the z-direction. Quantum transport properties of all the considered systems were calculated using the nonequilibrium Green's function formalism with the Brillouin zone sampled with (1, 1, 100) points. All simulations were conducted using the first-principles computational package Atomistix toolkit (ATK) [21].

III. RESULTS AND DISCUSSIONS

As a typical example, we study a graphene nanoribbon with zigzag edges. The edge atoms are terminated by hydrogen atoms to obtain better structural and electronic stability and saturates the carbon 2p states dangling bonds at the edges which give rise to localized states in the bare graphene nanoribbon. We consider single and double carbon substitutions by B, N and Si atoms either at the edges of the sample (Figs. 1(a, c)) or in the middle of the ribbon (Figs. 1(b, d)). In our device geometries, the size of the active layer was 24.61 Å and the size of the electrodes was 7.38 Å. After optimization, B and N atoms stay in the same plane of graphene, whereas a small vertical displacement is obtained for Si atoms due to their larger atomic radius.

We start by considering the effect of single carbon substitution on the electronic transport in the graphene nanoribbon. Figure 2 shows the zero-bias transmission spectra (a) and device density of states (DDOS) (b) as a function of the electronic energy for samples with edge doping. Solid-black curves show the results for pristine graphene as a reference. In the latter case, $T(E)$ exhibits a sequence of steps of integer transmission and an enhanced transmission at the Fermi level, which are typical for graphene nanoribbons (see solid-black curve in Fig. 2(a)). This feature in the transmission spectrum originates from the edge-localized electronic states with energies close to the Fermi energy. The transmission spectrum changes drastically when B and N atoms substitute the edge carbon atoms (dashed-red and dotted-green curves). $T(E)$ becomes smaller at the Fermi level and it drops sharply with increasing (decreasing) electron energy away from the Fermi energy for B and N doping. In fact, electrons can be totally reflected at these small energies. Interestingly, the obtained minima in the transmission curves are reflected in the DDOS as broad maxima at the same electron energies (see dashed-red and dotted-green curves in Fig. 2(b)). However, the Si-doped sample does not show such reduction in the electron transmission, except for a small local minima at larger electron energy. Thus, for edge terminated samples Si-doping results in better electron transmission in the graphene nanoribbons.

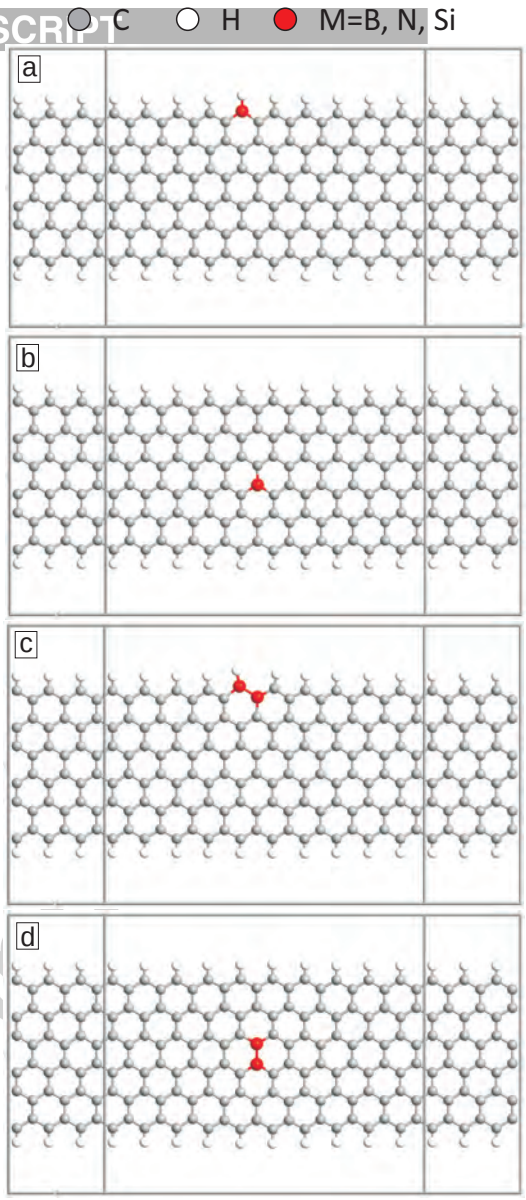

FIG. 1: (Color online) Device geometries: hydrogen passivated graphene nanoribbons with single (a, b) and double (c, d) substitutional doping at the edge (a, c) and at the center (b, d). Substitutions are performed with B, N and Si.

In order to understand the origin for the obtained changes in the transmission spectrum due to the atomic substitutions, we calculated the projected self-consistent Hamiltonian (PSH) eigenstates of all systems at different energies. The PSH eigenstates are associated with the poles of the Green's function and correspond to the peaks in the transmission spectrum. Insets in Fig. 2(b) show the PSH eigenstates corresponding to the energy levels near the transmission minima (indicated by vertical lines in Fig. 2(a)). In both cases, the electronic

ACCEPTED MANUSCRIPT

states are localized near the electrodes. Such nanoscale charge localizations are known to reduce the probability of electron transmission. No charge localizations are obtained for the Si-doped sample for this range of energy (not shown here) and therefore we obtain larger electron transmission.

Figure 3 shows the result obtained for the samples with center substitutional doping. The B and N doped samples shows very similar transmission spectra as in the case of the edge-doped samples. The only difference is that the location of the minima in the transmission is shifted further away from the Dirac point for both samples. Profound minima in the transmission spectrum is also obtained for the Si-doped sample, which also originates from the strong localization of the electronic states in the system (see the inset in Fig. 3(b)). Again, all the minima in the transmission spectra are reflected in the DDOS as a local maxima (Fig. 3(b)). Since the location of the minima in the transmission curves is further away from the Fermi energy for the Si-doped sample, we can again conclude that Si substitution results in better electronic transport in this system as compared to the other systems.

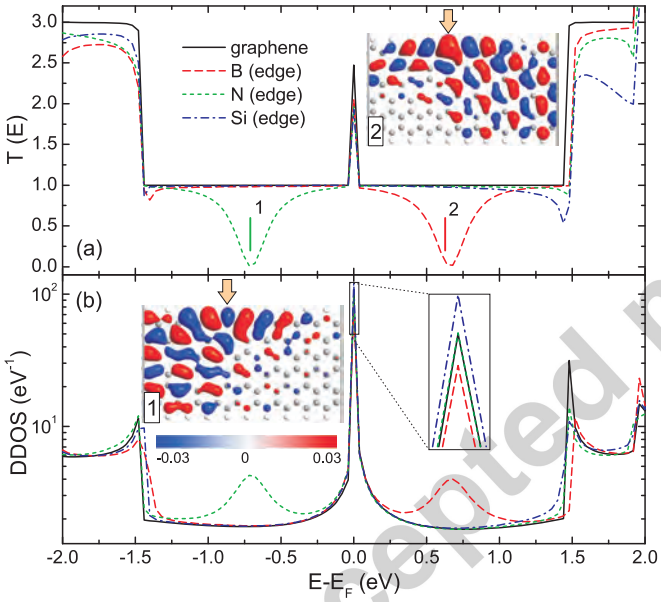

FIG. 2: (Color online) (a) Zero bias transmission spectra ($T(E)$) and (b) device density of states (DDOS) as a function of electron energy. Energy origin coincides with the Fermi energy. The results are shown for a pristine graphene ribbon (solid-black curves) and for graphene with a single edge substitution with B (dashed-red curves), N (dashed-green curve) and Si (dash-dotted blue curve) atoms. Insets 1 and 2 show isosurface plots of the projected self-consistent hamiltonian eigenstates of the samples with N substitution (inset 1) and B substitution (inset 2) corresponding to the energy levels indicated by the vertical lines in Fig. 1(a). Arrows in these insets indicate the position of the carbon substitution. The increase of DDOS near the Fermi level is given in the other inset of Fig. 2(b).

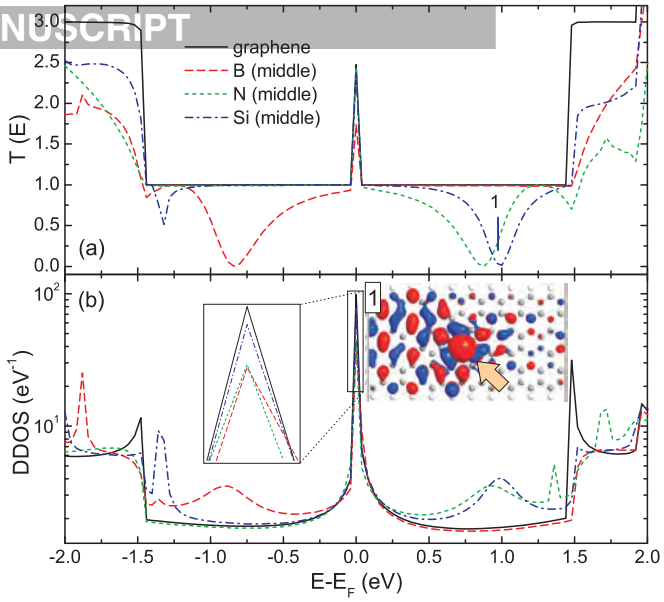

FIG. 3: (Color online) The same as Fig. 1, but the substitutional doping is in the middle of the sample. Inset 1 shows the isosurface plot of the projected self-consistent hamiltonian eigenstates for the Si-doped sample. The enlargement of the device density of states near the Fermi level is given in the other inset of Fig. 3(b).

In order to see the contribution of the dopant atoms to the density of states (DOS) of the system, we have calculated the projected DOS of the graphene nanoribbon with a single doping atom. Figure 4 shows the DOS of pristine graphene nanoribbon (see the inset in Fig. 4(a)) projected on the C and H atoms. It is seen from this figure that the DOS is dominated by the p-states of the C

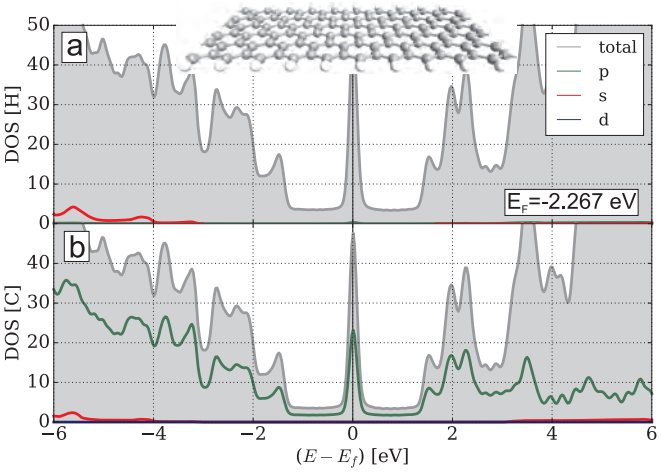

FIG. 4: (Color online) Density of states of pristine graphene nanoribbon projected on the H (a) and the C (b) atoms. Energy origin is set to coincide with the Fermi level. The number reports the value of the Fermi energy. Inset in (a) shows the optimized structure of the graphene nanoribbon.

Accepted manuscript

ACCEPTED MANUSCRIPT

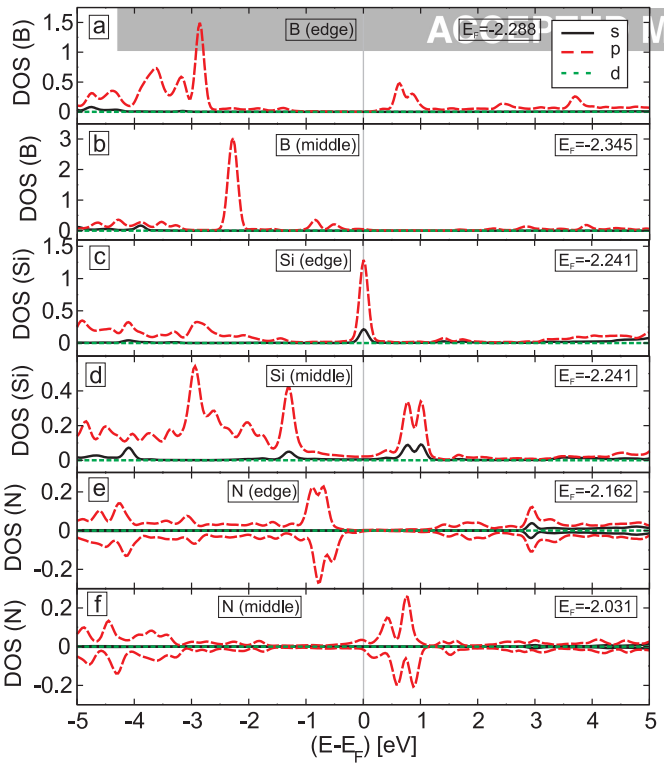

FIG. 5: (Color online) Density of states of graphene nanoribbon with a single doping atom at the edge (a, c, e) and in the middle of the ribbon (b, d, f) projected on B (a, b), Si (c, d) and N (e, f) atoms. Energy origin is set to coincide with the Fermi level. The value of the Fermi energy is shown in each panel.

atoms with smaller contributions from the *s*-states deep inside the valence band (Fig. 4(b)). The contribution of the terminating H atoms are also obtained away from the Fermi level (Fig. 4(a)).

Figure 5 shows the DOS of the graphene nanoribbon substitutionally doped with a single foreign atom projected on the dopant atom. In the case of the edge B-doping (Fig. 5(a)), the contribution of the B atom is obtained at the energy ∼0.75 eV above the Fermi level. This is the value of the energy for which we have observed reduced transmission (see Fig. 2(a)). The contribution of the B atoms in the valence band is found further away from the Fermi level. In the case of B doping in the middle of the ribbon (Fig. 5(b)), the largest contribution of dopant atom is obtained in the valence band, where reduced transmission was reported (see Fig. 3(a)). For the edge Si doping, the largest contribution of the Si atom orbitals to the DOS is obtained at the Fermi level (Fig. 5(c)). This is also reflected in the device density of states (see the inset in Fig. 2(b)). The contribution of the Si atom becomes less pronounced away from the Fermi energy. For the energy interval [-2 eV, 2 eV], for which we have calculated the transmission spectrum, two peaks are obtained in the case of the middle Si doping (Fig. 5(d)). Both of these peaks correspond to reduced transmission in the system (see Fig. 3(b)). Finally, Figs. 5(e, f) shows the contribution of the electronic states of the N atom to the DOS of the system. The position of the maxima in the projected DOS depends on the location of the dopants and always corresponds to the reduced electronic transmission (see Figs. 2(a) and 3(a)). Note that due to the spin degeneracy, we have calculated spin dependent DOS for N-doped systems. The Fermi energies of the considered systems also depend on the type and location of the dopants. For example, the *p*-type B doping decreases the Fermi level, whereas *n*-type N doping results in an increase of the Fermi energy (see the numbers in Fig. 5). The largest shift is obtained for doping in the middle of the sample. Substitutional doping with Si atoms slightly increases the Fermi level of the system independently of the impurity location. These findings show the importance of the difference in the number of valence electrons of the dopant atoms.

Next, we consider the case of double carbon substitutions but only dimer impurities are considered, impurities are put at adjacent sites and hence we do not aim to probe impurity-impurity correlation effects. As our main results, we show in Fig. 6 the zero-voltage transmission spectra of the sample for edge (a) and center (b) substitutional doping. For the B and N edge-doping (Fig. 6(a)), at least 4 minima are obtained in the transmission spectra in the energy interval of [-1.5, 1.5] eV, which was not the case for single doping (see Fig. 2(a)). Some of the minima are very close to the Fermi energy which are responsible for the considerable reduction of the electron transmission in the experimentally relevant range of en-

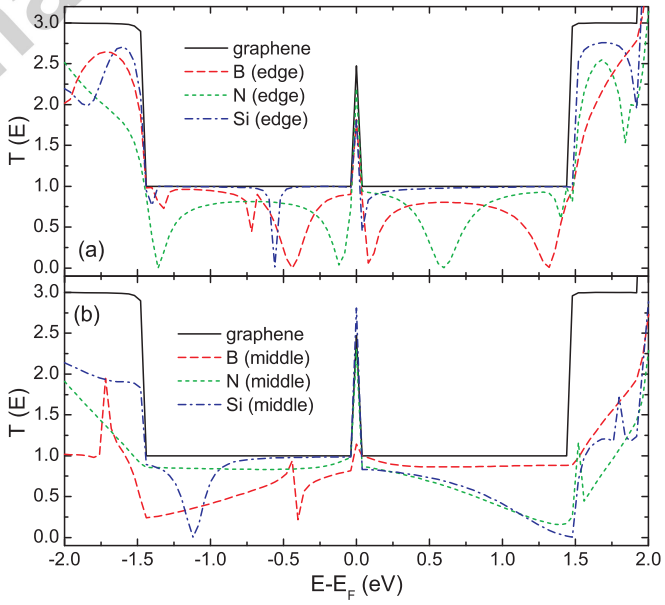

FIG. 6: (Color online) Zero-bias transmission spectra of graphene nanoribbons with double carbon substitutions at the edge (a) and in the middle (b) of the sample. The results are shown for B (dashed-red curves), N (dotted-green curves) and Si (dash-dotted blue curves) substitutions.

Accepted manuscript

ACCEPTED MANUSCRIPT

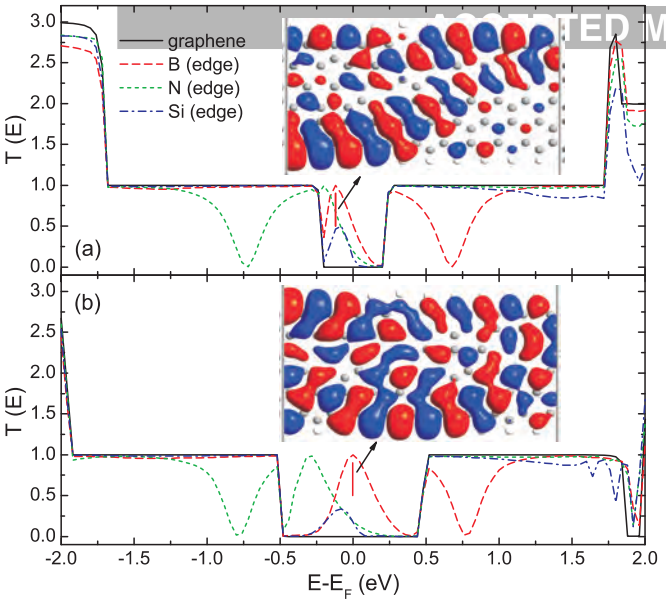

FIG. 7: (Color online) Transmission spectra of graphene nanoribbons with single edge atomic substitution for finite voltage biasing with $\Delta V = 0.5$ V (a) and $\Delta V = 1$ V (b). Insets show isosurface plots of the projected self-consistent hamiltonian eigenstates of the samples with B substitution corresponding to the energy levels indicated by the red vertical lines.

ergies. These minima in the transmission spectra also originate from localized electronic states in the system (not shown here). Si-doped sample shows two minima in the same range of energy. However, these minima are much narrower than the ones obtained for the other two samples. This again indicates that Si-doping does not affect much the transport properties of graphene. Finally, Fig. 6(b) shows transmission spectra for double carbon substituted samples in the middle of the nanoribbon. Qualitative changes are obtained in the transmission spectra as compared to the edge-doped samples. For example, most of the minima in the transmission spectra near the Fermi energy disappear for all the considered samples. This indicates the importance of edge states in the electronic transport in graphene nanoribbons. Still, the Si-doped sample shows better electronic transport as compared to the other two samples. In fact, the transmission in the latter sample at the Fermi level is larger than the transmission in pristine graphene.

In what follows, we study the effect of voltage biasing on the electronic transport in doped-graphene nanoribbons. Figure 7 shows the transmission spectra of all considered samples with single edge doping for the voltage difference $\Delta V = 0.5$ V (a) and $\Delta V = 1$ V (b). For the pristine graphene nanoribbon (solid-black curve in Fig. 7(a)), zero transmission is obtained near the Fermi level, which is due to the finite gap opening in the band structure of the system under voltage biasing. This region increases with increasing applied voltage (Fig. 7(b)). However, for the doped samples a finite transmission is still observed for both values of the applied voltage near the Fermi level. The other minima in the transmission remain the same. The reason for such finite transmission is the formation of electronic states extended between the electrodes (see the insets in Fig. 7). The transmission near the Fermi energy is now larger for the B-doped sample. Similar results were obtained for samples with carbon atoms substituted in the middle of the nanoribbon, which are shown in Fig. 6 for two values of the applied voltage. However, the transmission near the Fermi energy is now smaller as compared to the case of the samples with impurity edge-substitution.

IV. CONCLUSION

First-principles DFT calculations in combination with the nonequilibrium Green's functional formalism have been performed to study the effect of substitutional doping on the transport properties of hydrogen terminated zig-zag nanoribbons. We used B, N and Si atoms for substituting carbon atoms either at the edge or in the middle of the sample. Despite similar, or even smaller DOS, Si-doped samples show better transmission as compared to the other two samples. The obtained results depend also on the location of the substitutional impurity. For example, better transmission is obtained for edge doping in the case of single substitutions, whereas doping in the middle of the sample gives better transmission in the case of double substitutions. The obtained changes in the transmission spectra due to the doping originates from the charge localizations in the system. Our results give insight in the effect of positional and elemental doping of

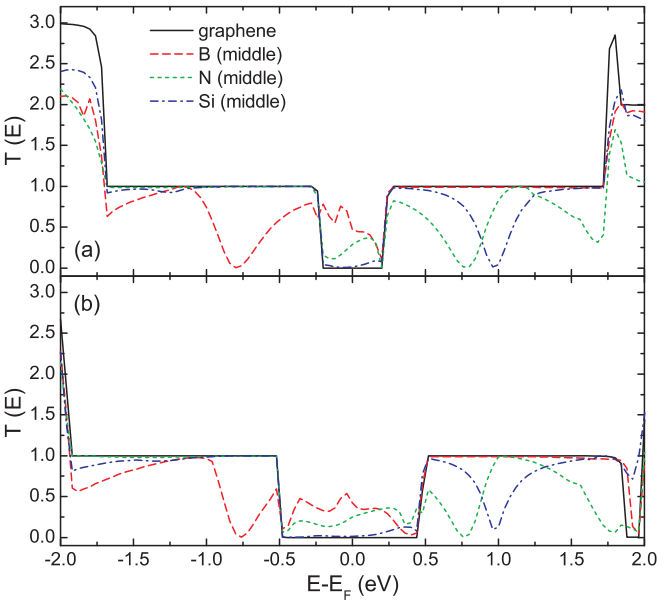

FIG. 8: (Color online) The same as Fig. 7, but now the substitutional doping is in the middle of the sample.

Accepted manuscript

ACCEPTED MANUSCRIPT

graphene nanoribbons. It will guide experimentalists to optimize the effect of doping.

V. ACKNOWLEDGEMENTS.

H. B. and F. M. P. acknowledge the support from King Fahd University of Petroleum and Minerals, Saudi Arabia, under research group project RG1329-1 & RG1329-2. G. R. B. acknowledges fruitful discussions with Dr. M. E. Madjet from Qatar Environment and Energy Research Institute.

[1] K. S. Novoselov, A. K. Geim, S. V. Morozov, D. Jiang, Y. Zhang, S. V. Dubonos, I. V. Grigorieva and A. A. Firsov, Science **306**, 666 (2004).
[2] A. K. Geim and K. S. Novoselov, Nat. Mater. **6**, 183 (2007).
[3] A. K. Geim, Science **324**, 1530 (2009).
[4] C. Neto, F. Guinea, N. M. R. Peres, K. S. Novoselov, and A. K. Geim, Rev. Mod. Phys. **81**, 109 (2009).
[5] K. Ratinac, W. Yang, S. P. Ringer, and F. Braet Environ. Sci. Technol. **44**, 1167 (2010).
[6] F. Xia, V. Perebeinos, Y. M. Lin, Y. Wu, and P. Avouris, Nat. Nanotechnol. **6**, 179 (2011).
[7] F. Schedin, A. K. Geim, S. V. Morozov, E. W. Hill, P. Blake, M. I. Katsnelson, and K. S. Novoselov, Nat. Mater. **6**, 652 (2007).
[8] K. S. Novoselov, A. K. Geim, S. V. Morozov, D. Jiang, M. I. Katsnelson, I. V. Grigorieva, S. V. Dubonos, and A. A. Firsov, Nature (London) **438**, 197 (2005).
[9] X. Wang, X. Li, L. Zhang, Y. Yoon, P. K. Weber, H. Wang, J. Guo, and H. Dai, Science **324**, 768 (2009).
[10] D. C. Wei, Y. Q. Liu, Y. Wang, H. L. Zhang, L. P. Huang, and G. Yu, Nano Lett. **9**, 1752 (2009).
[11] B. D. Guo, Q. Liu, E. Chen, H. W. Zhu, L. Fang, and J. R. Gong, Nano Lett. **10**, 4975 (2010).
[12] Z. F. Wu, W. C. Ren, L. Xu, F. Li and H. M. Cheng, ACS Nano, **5**, 5463 (2011).
[13] H. Xiao, Y. Chen, Y. Xie, T. Ouyang, Y. Zhang, and J. Zhong, J. Appl. Phys. **112**, 113713 (2012).
[14] Y. An, X. Wei, and Z. Yang, Phys. Chem. Chem. Phys., **14**, 15802 (2012).
[15] Y. An, X. Wei, and Z. Yang, Phys. Rev. B **80**, 235426 (2009).
[16] B. I. Zhou, B. H. Zhou, X. W. Chen and G. H. Zhou, Eur. Phys. J. B**85**, 121 (2012).
[17] X.H. Zheng, I. Rungger, Z. Zeng and S. Sanvito, J. Appl. Phys. **109**, 124502 (2011).
[18] J. P. Perdew, K. Burke, and M. Ernzerhof, Phys. Rev. Lett. **77**, 3865 (1996).
[19] H. J. Monkhorst and J. D. Pack, Phys. Rev. B **13**, 5188 (1976).
[20] S. Grimme, J. Comp. Chem. **27**, 15 (2006).
[21] Distributed by QuantumWise company, Copenhagen, Denmark. http://www.quantumwise.com.

Accepted manuscript